Semiconductors, 2023, Vol. 57, No. 8

Lateral mode selection of single-mode laser diode microstripe bar (1050 nm) in external cavity

© A.A. Podoskin, I.V. Shushkanov, A.E. Rizaev, M.I. Kondratov, A.E. Grishin, S.O. Slipchenko

Ioffe Institute,
194021 St. Petersburg, Russia

E-mail: podoskin@mail.ioffe.ru

Received November 17, 2023
Revised December 4, 2023
Accepted December 4, 2023

Radiative characteristics of microstripe laser diode bar in an external resonator based on an aspherical lens and a flat dielectric mirror were Investigated. The bar had total emitting aperture of 185 μm, formed by 10 stripes with a width of 6 μm separated by mesa-grooves. Operation in the external resonator of the entire emitting aperture was characterized by a multimode generation regime with a peak power of 3 W/6 A. Selection of lateral modal structures and transition to a single-mode regime is possible by limiting the number of stripes involved in optical feedback. Dependences of optical mode reconfiguration were studied by introducing limiting slits into the external cavity. It was shown that limiting the emitting aperture involved in the feedback to 65 μm allows us to demonstrate high-order single-mode operation with far-field divergence for the central lobe of 1°.

Keywords: laser bar, external cavity, high-order single-mode.

DOI: 10.61011/SC.2023.08.57623.5763

1. Introduction

Currently, one of the conditions for increasing the efficiency of using high-power semiconductor lasers to solve practical applied problems is to obtain a laser beam with high optical quality. Classic semiconductor laser emitters based on stripe designs are limited by the multimode nature of the radiation that arises when using wide emitting apertures [1,2]. As an alternative, both to obtain high beam quality and to increase the yield power, various design options for emitters have been proposed: integral resonant cavities [3–5], integral [6,7] and discrete [8,9] Master Oscillator Power Amplifier (MOPA)-designs, circuits based on an external resonant cavity [10–13]. A condition for achieving high quality laser beam is the operation of a broad area laser in a common optical mode. The implementation of this principle makes it possible to radically reduce the divergence (to $< 1°$ values) and increase the radiance. One of the design options for solving the problem of improving the quality of the optical beam is the use of bars based on individual single-mode waveguides with optical coupling between them [14]. The ground problem in this case is the generation of unwanted high-order mode structures arising due to the low lateral mode selectivity of the laser array's own Fabry–Perot resonant cavity. The use of an external optical resonant cavity will provide both effective coupling between individual lateral waveguides and selection with suppression of unwanted mode structures and operation on one common lateral mode.

2. Experimental samples and methodologies of studies

Samples of microarrays of single-mode lasers were made on the basis of a heterostructure with asymmetric emitters and the location of the active region. The heterostructure consisted of an $Al_xGa_{1-x}As$ ($x = 10\%$) waveguide with a thickness of 1.5 μm, limited by wide-gap emitters n-$Al_xGa_{1-x}As$ ($x = 15\%$) and p-$Al_xGa_{1-x}As$ ($x = 35\%$). The active region based on two InGaAs quantum wells ($\lambda = 1050$ nm) was located in the waveguide layer at a distance of 0.2 μm from the p-emitter. The heterostructure was grown by metal-organic compound (MOC)-hydride epitaxy. To measure the general emission characteristics, samples of multimode lasers of a mesa-strip design with an aperture width of 100 μm were manufactured from this heterostructure. At pumping with a continuous current, internal optical losses of 0.53 cm^{-1} and an internal quantum efficiency of 97% were demonstrated. In this case, the transparency current was 100 A/cm^2. The radiation pattern in a plane perpendicular to the layers of the heterostructure had an 24° divergence at full width half maximum (FWHM) and was stable over a wide range of pumping currents. Next, samples of micro-arrays of single-mode lasers were manufactured. The microruler contained 10 strips, each 6 μm wide, which were separated by mesa-grooves 14 μm wide. The total width of the microruler was 185 μm. The depth of the dividing groove was chosen consistently during numerical simulation, based on two requirements: (1) ensuring generation on the fundamental lateral optical mode of a separate isolated strip, (2) providing the required value of the optical coupling parameter between the nearest microruler strips. The fulfillment of the second condition is also due to the sensitivity of the formed refraction index profile to changes in the operating temperature and pumping current amplitude. The choice of groove depth is a compromise between the requirement for a refraction index profile that would form a lateral waveguide that is robust to variations in pumping current and temperature, and also provide the ability to obtain an optically coupled lateral mode structure when operating from an external resonant cavity. Thus, in the work [14] it was shown that the value of the optical coupling parameter $\leq 10^{-5}$ ensures independent generation of stripes in a microruler, without traces of common lateral mode structures. As a result , the optical communication parameter $\leq 8 \cdot 10^{-6}$ was chosen in this work. For experimental studies of the operating features of a microruler in an external resonant cavity, samples of microrulers with a crystal length of 2 mm were manufactured. Reflective ($R = 5\%$ for the yield end) and antireflective ($R < 1\%$ on the side of the external resonator) coatings were applied to the end faces of the microrulers, which form their own Fabry–Perot resonant cavity.

To study the generation features and characteristics of the general mode structures of the microbar, we used an external resonant cavity circuit (Figure 1) based on a flat dielectric mirror with a reflectance of 99.5%, which was located on the side of the face with a reflectance $R < 1\%$. The collimation of the microruler radiation beam directed to the mirror and the reverse input of the reflected beam were carried out by one aspherical lens with a numerical aperture $NA = 0.5$ and a focal distance $f = 8$ mm. This choice was determined by the desire to create an optical design with a minimum number of elements, which would be as simple as possible for implementation and adjustment. The length of the externa resonant cavity in the experiment was chosen to be 70 mm. Experiments have shown that the selected value provides satisfactory stability of the optical circuit to mechanical vibrations and misalignment. The mode structure of the lateral waveguide of the microruler in the considered external resonant cavity circuit was controlled by: (1) lateral adjustment of the microruler relative to the collimating lens (along the y axis in Figure 1); (2) introducing additional opaque screens into the optical beam between the microruler and the dielectric mirror (Figure 1). Samples of microrulers were placed on a thermally stabilized copper heat sink and pumped by rectangular current pulses with a duration of 400 ns. The experiments were carried out at temperature of 20°C. As part of the experimental studies, measurements of the distribution of radiation intensity in the near and far zones were carried out. To measure the intensity distribution in the near zone using an optical system, an enlarged image of the yield mirror plane was constructed and the intensity was measured using a CCD camera. To analyze the angular distribution of lateral modes in the far zone, a beam collimated in a plane perpendicular to the layers of the heterostructure was formed using an optical scheme. The intensity distribution in the beam was determined using a CCD camera at a distance of 35 mm from the lens. In this configuration of the optical scheme for recording radiation, the linear lateral size of the optical beam reflects its divergence. This far-field analysis scheme makes it possible to effectively adjust the feedback in the resonant cavity simultaneously with recording the parameters of the yield radiation.

3. Experimental results and discussion

Experiments on mode selection in an external resonant cavity were carried out in two intervals. At the first interval of the experiment, a resonant cavity circuit without limiting screens was used. In this diagram, the influence of lateral adjustment on the lateral mode structures formed in the external resonant cavity was studied. When operating a microline crystal in an external resonant cavity, changing the lateral position of the sample relative to the optical axis of the external resonant cavity circuit allowed to consistently implement feedback conditions for any given number of groups of nearby strips from 1 to 10 (along the axis y Figure 1). To eliminate the influence of Fabry–Perot resonant cavity modes, when analyzing the behavior of the profile of the yield optical beam with optical feedback for a different number of strips, a pump current of 1.6 A was chosen, the value of which is lower than the lasing threshold of the microruler crystal without feedback from the external

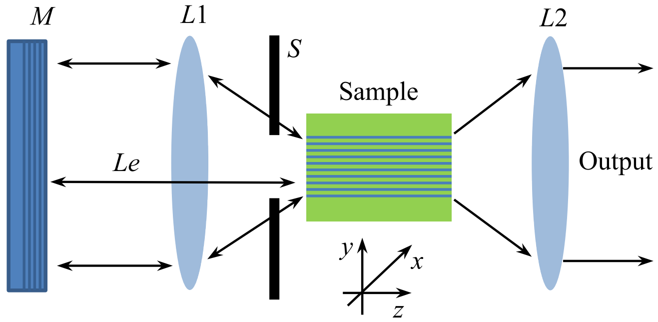

Figure 1. General view of the experimental circuit of an external resonant cavity. $L1$ and $L2$ — collimating lenses, M — external mirror, S — limiting screen, Le — length of external resonant cavity.

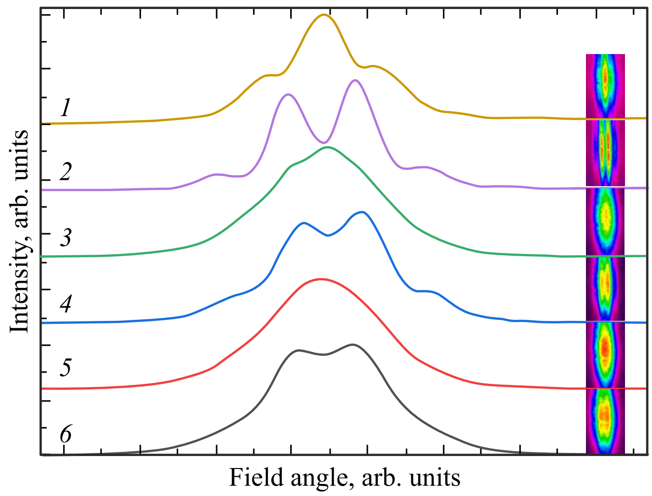

Figure 2. Intensity distributions of the yield radiation of a microbar in the far field for the cross section of a collimated yield beam at a pumping current of 1.6 A and the presence of feedback for a different number of strips: *1* — 1, *2* — 2, *3* — 5, *4* — 6, *5* — 9, *6* — 10. Insets show two-dimensional intensity distributions of a collimated beam at a distance of 35 mm from the collimating lens. (The colored version of the figure is available on-line).

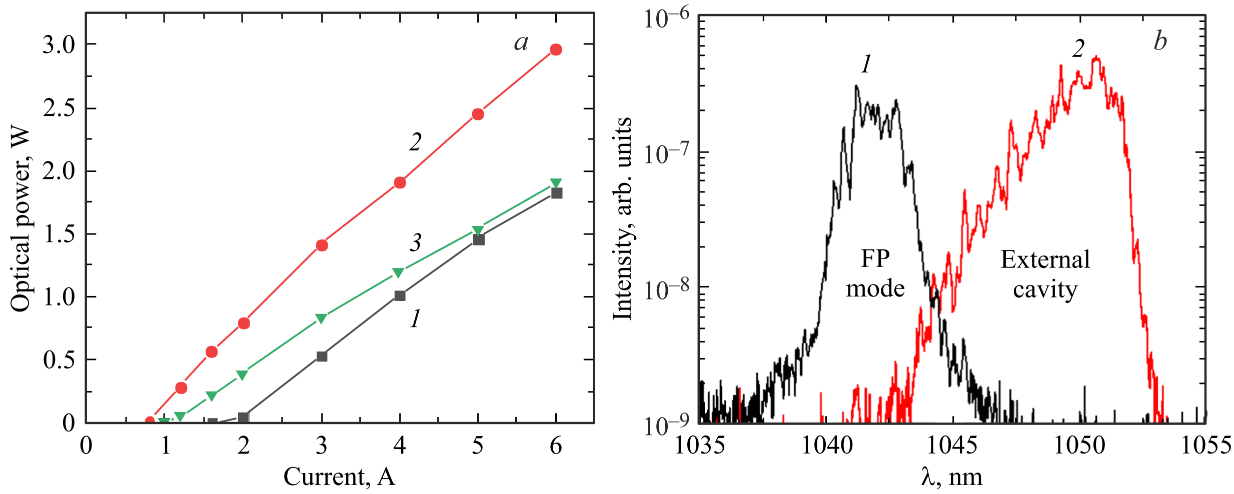

Figure 3. *a* — dependence of the peak yield optical power on the amplitude of the pumping current; *b* — laser emission spectra for a pumping current of 6 A for various resonant cavity designs: *1* — own Fabry–Perot resonant cavity without feedback in an external resonant cavity; *2* and *3* — with feedback in an external resonant cavity for all 10 microruler strips without and with limiting screens, respectively.

resonant cavity, i. e., on modes of the own Fabry–Perot resonant cavity (as will be shown below, the threshold of the own Fabry–Perot resonant cavity reaches 2 A). As a result, there were features of two types (Figure 2). First, the shape of the lateral mode depended on the number of stripes involved in the feedback of the external resonant cavity. For an odd number of stripes, there was a symmetrical shape of the lateral intensity distribution profile in the far zone with an intensity maximum in the center of the radiation pattern („even“ mode). For an even number of stripes, the shape had a central local minimum of intensity („odd“ mode). Secondly, with an increase in the number of stripes involved in feedback, there is a broadening of the lobes of the lateral far field. We associate such broadening with an increase in the number of uncoupled lateral mode structures simultaneously operating in the external resonant cavity, i. e. with the transition to a multimode lasing regime.

Let us review in more detail the features of the microruler with feedback for all 10 strips. Samples of microrulers with coated end faces in the absence of feedback in the external resonant cavity demonstrated the mode generation threshold of the Fabry–Perot resonant cavity ~ 2 A. In this case, the slope of the watt-ampere characteristic (WAC) was 0.48 W/A (Figure 3, *a*), and the maximum of the generation spectrum was located in the region of 1042 nm for a current amplitude of 6 A (Figure 3, *b*). The transition of the microbar operation from the mode of its own Fabry–Perot resonant cavity to operation in an external resonant cavity for all 10 strips allowed to reduce the threshold to 800 mA and increase the slope of the Watt characteristic to 0.54 W/A (Figure 3, *a*). In this case, the yield optical power reached 3 W at a pump amplitude of 6 A. The laser emission spectrum (Figure 3, *b*) for a microarray operating in an external resonant cavity demonstrates a significant shift to long wavelengths: a maximum in the region of 1051 nm for a pumping current amplitude of 4 A. The shift of the laser emission spectrum to the long-wavelength region indicates a decrease in optical losses, which requires a lower threshold gain and, as a consequence, a lower carrier concentration in the active region of the microruler strips. However, for samples of rulers with *AR–HR* mirrors with reflectance of 97 and 5%, the slope was 0.82 W/A, i.e. in a circuit with an external resonant cavity, despite the appearance of optical coupling between the strips of the ruler, there is no complete reduction of the radiative efficiency.

From Figure 4 it is clear that in the distribution of radiation intensity in the near zone when operating in an external resonant cavity circuit, the lateral mode structure fills not only the areas under the pumped strips, but also the areas under the non-pumped separating mesogrooves. On the one hand, this indicates the efficiency of the external resonant cavity from the point of view of obtaining a common lateral mode structure that optically connects all strips of the microline. On the other hand, the presence of intense laser lasing in the mesa-groove regions that are not pumped by current allows us to conclude that there are additional optical losses for the overall lateral mode structure of the microbar compared to the modes of the *AR–HR* emitter without effective optical coupling between the strips, which also contributes to the reduction radiative efficiency when working with an external resonant cavity.

At the second interval of the experiment, additional absorbing screens were added to the external resonant cavity circuit between the microruler sample and the collimating aspherical lens (Figure 1), limiting part of the radiation pattern in the lateral plane, which made it possible to study the effect of the screens on mode selection in the external resonant cavity. The original external resonant cavity circuit was configured to operate with feedback from all ten strips in the external resonant cavity, with a pumping current of 1.6 A/400 ns. The observed profile of the collimated

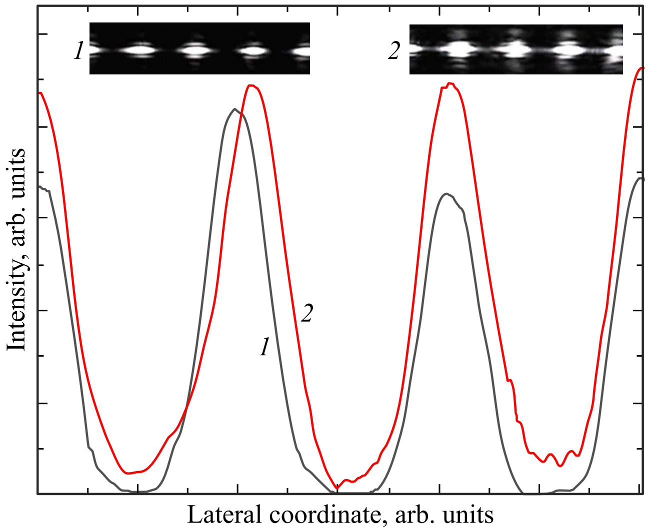

Figure 4. Enlarged image of the intensity distribution of the yield radiation of a microline in the near zone on the yield face for the central region of the microline at a pumping current of 6 A/400 ns: *1* — without external feedback, *2* — with external feedback for 10 strips. The inserts show two-dimensional radiation intensity distributions on the yield mirror of the microruler.

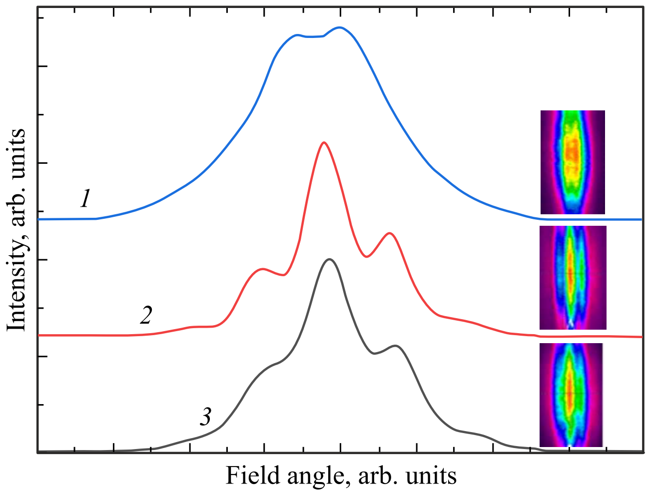

Figure 5. Intensity distributions of the oyield radiation of the microruler in the cross section of the collimated yield beam: *1* — without an external resonant cavity at a pumping current of 6 A; in an external resonant cavity circuit providing feedback for all 10 strips in the presence of a two-sided symmetrical lateral limiting screen at pumping currents A: *2* — 2, *3* — 6. Insets show two-dimensional intensity distributions of a collimated beam at a distance of 35 mm from the collimating lens. (The colored version of the figure is available on-line).

beam cross section (Figure 5) demonstrates a narrowing of the intensity distribution in the far zone, which indicates a higher lateral mode selectivity compared to the case of operation of an external resonant cavity without screens (Figure 2, case for 10 strips). It also follows from Figure 5 that the nature of generation in the microarray is lateral multimode, and with increasing pumping amplitude the mode selectivity deteriorates. The dependences of the yield optical power on the pumping amplitude for the operating mode with limiting screens are shown in Figure 3, *a*. It can be seen that the achieved power for a current of 6 A was 1.7 W, which is significantly lower than the value obtained for the circuit without limiting screens, and is comparable to the value achieved when the line operates without an external resonant cavity. However, the threshold currents achieved when operating in an external resonant cavity with limiting screens were 1050 mA, which is slightly higher than in the circuit without screens and noticeably lower than for the operating mode without an external resonant cavity. This indicates that the radiative efficiency of a circuit with an additional screen is significantly lower than for the case without it (Figure 3, *a*, dependences 1 and 2). Thus, confining screens not only increase lateral selectivity, but also introduce additional intracavity optical losses for some operating modes.

To study the influence of limiting screens on the mode selection of the external resonant cavity, the distance between symmetrically located screens was reduced. As a result, the lateral size of the area with effective feedback was significantly reduced. This led to a reduction in the number of strips operating in the external resonant cavity to 4; at the same time, the divergence of the lateral field in the far zone became even narrower (Figure 6). Removal of one of the screens caused a symmetrical expansion of the area of the microruler covered by feedback. In the example given, the number of strips operating in the external resonant cavity has increased to 6, and the lateral far field also expands. As a result, it is shown (Figure 6) that the introduction of screens limits part of the radiation pattern in the lateral plane. At the same time, the feedback region for the microruler strips is reduced from 10 to 4 (region width 65 μm) and operation on a single lateral mode, albeit of a higher order, is ensured.

At the final interval of the research, the influence of lateral adjustment on mode selection in an external resonant cavity circuit with an optimal arrangement of additional limiting screens was considered. To demonstrate the angular divergence, in the final part of the research, measurements of the angular distribution of the far field were carried out (Figure 7, *a*). As was shown earlier (Figure 6), adding screens allows to achieve a lateral single-mode lasing mode. Additional lateral adjustment (along the y axis in Figure 1) of the position of the microruler sample relative to the optical axis of the external resonant cavity circuit ensures stable generation in a single-mode either on the even or odd common lateral mode (Figure 7, *a*) while maintaining the general shape of the radiation intensity distribution in the near zone (Figure 7, *b*). It is also clear from the presented dependences that the total lateral divergence of radiation in the case of operation with an external resonant cavity is comparable to that for the mode of operation on Fabry–Perot resonant cavity modes without feedback, which

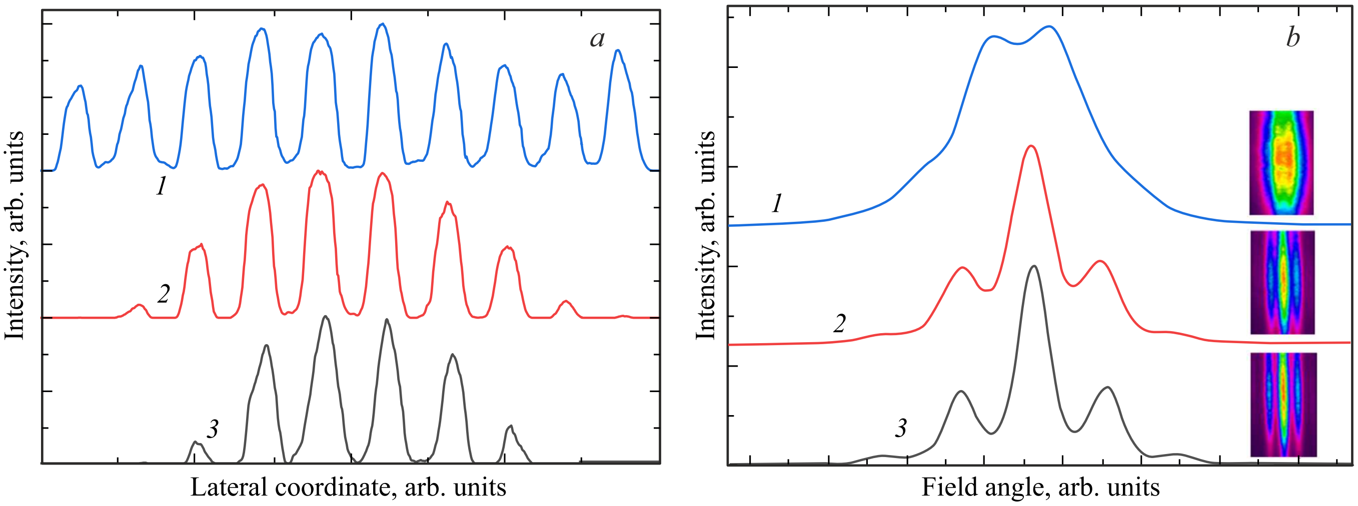

Figure 6. Intensity distributions of the yield radiation of the microbar: *a* — on the yield face („near zone") and *b* — in the cross section of the collimated yield beam in the external resonant cavity circuit with feedback for 10 strips with a pumping current of 1.6 A and the addition of lateral limiting screens: *1* — without screens, *2* — one-sided screen, *3* — two-sided symmetrical screen. Insets show two-dimensional intensity distributions of a collimated beam at a distance of 35 mm from the collimating lens. (The colored version of the figure is available on-line).

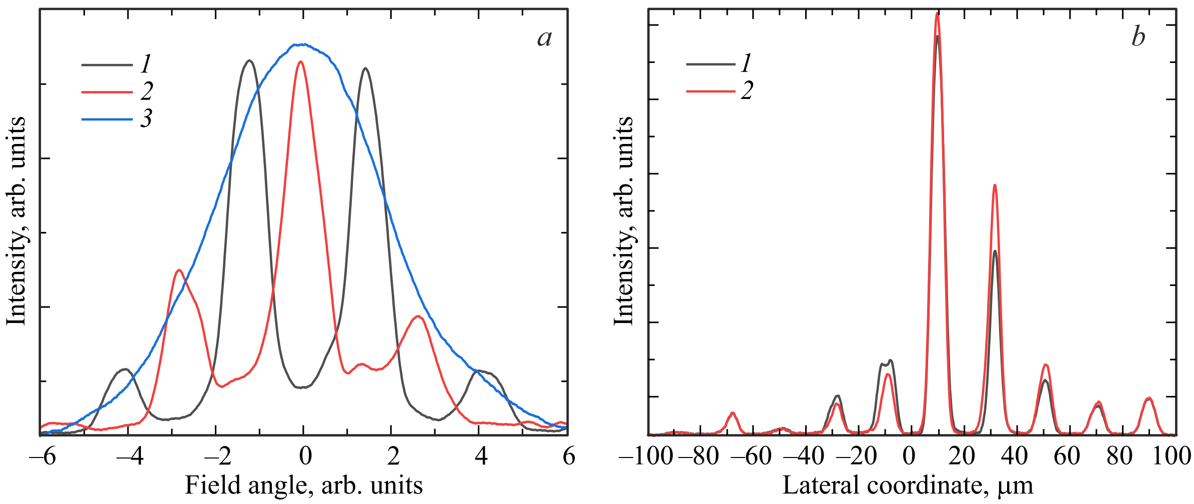

Figure 7. Intensity distributions of the yield radiation of a microbar in an external resonant cavity circuit with feedback in the presence of a two-sided symmetrical lateral limiting screen at a pumping current of 2.3 A: *a* — in the far zone (directional pattern), *b* — in the near zone (at the yield end) for two options for lateral adjustment (along the *y* axis of Figure 1): *1* — even mode with a minimum in the center, *2* — odd mode with a maximum in the center, *3* — own Fabry–Perot resonant cavity without external feedback.

amounted to 4.6° at half maximum. In this case, for the external resonant cavity, the width of the individual lobes of the radiation pattern is $\sim 1°$ at half maximum.

4. Conclusion

Using an external resonant cavity with a total length of 70 mm, optical feedback from an external flat mirror was demonstrated for the entire width of a microruler — 185 μm, formed by a periodic structure of 10 single-mode mesa-stripes arranged with a period of 20 μm. It is shown that in the considered external resonant cavity circuit, the emerging lateral mode structure has a single-mode character (high-order mode) for the feedback 4 strip and a multimode character for the entire width of the line of 10 strips. This allows to assert that when constructing an optical circuit of an external resonator based on aspherical optics, the optimal width of the microruler, for which mode selection and single-mode operation are realized, reaches 65 μm. To increase the optical power within a given value of the total aperture, designs with a smaller width of the limiting mesa-grooves can be reviewed in the future.

Acknowledgments

The authors would like to thank P.S. Gavrina for her assistance in preparing the publication materials.

Conflict of interest

The authors declare that they have no conflict of interest.

References

[1] S.O. Slipchenko, D.A. Veselov, V.V. Zolotarev, A.V. Lyutetskii, A.A. Podoskin, Z.N. Sokolova, V.V. Shamakhov, I.S. Shashkin, P.S. Kop'ev, N.A. Pikhtin. Bull. Lebedev Phys. Inst., **50**, S494 (2023). DOI: 10.3103/S1068335623160108
[2] P. Crump, G. Erbert, H. Wenzel, C. Frevert, C.M. Schultz, K.-H. Hasler, R. Staske, B. Sumpf, A. Maaßdorf, F. Bugge, S. Knigge, G. Tränkle. IEEE J. Select. Topics Quant. Electron., **19**, 1501211 (2013). DOI: 10.1109/JSTQE.2013.2239961
[3] B. Sumpf, K.H. Hasler, P. Adamiec, F. Bugge, F. Dittmar, J.Ö. Fricke, H. Wenzel, M. Zorn, G.Ö. Erbert, G. Tränkle. IEEE J. Select. Topics Quant. Electron., **15**, 1009 (2009). DOI: 10.1109/JSTQE.2008.2010952
[4] G. Hergenhan, B. Lücke, U. Brauch. Appl. Optics, **42**, 1667 (2003). DOI: 10.1364/AO.42.001667
[5] M. Yoshida, S. Katsuno, T. Inoue, J. Gelleta, K. Izumi, M. De Zoysa, K. Ishizaki, S. Noda. Nature, **618**, 727 (2023). DOI: 10.1038/s41586-023-06059-8
[6] H. Wenzel, S. Schwertfeger, A. Klehr, D. Jedrzejczyk, T. Hoffmann, G. Erbert. Optics Lett., **37**, 1826 (2012). DOI: 10.1364/OL.37.001826
[7] H. Wenzel, K. Paschke, O. Brox, F. Bugge, J. Fricke, A. Ginolas, A. Knauer, P. Ressel, G. Erbert. Electron. Lett., **43**, 1 (2007).
[8] H. Wenzel, A. Klehr, S. Schwertfeger, A. Liero, T. Hoffmann, O. Brox, M. Thomas, G. Erbert, G. Tränkle. *Proc. Volume 8241, High-Power Diode Laser Technology and Applications X* (82410V, San Francisco, California, United States, 2012). DOI: 10.1117/12.906320
[9] S. Riecke, S. Schwertfeger, K. Lauritsen, K. Paschke, R. Erdmann, G. Tränkle. Appl. Phys. B, **98**, 295 (2010). DOI: 10.1007/s00340-009-3672-z
[10] M. Niebuhr, C. Zink, A. Jechow, A. Heuer, L.B. Glebov, R. Menzel. Opt. Express, **23**, 12394 (2015). DOI:10.1364/OE.23.012394
[11] A. Jechow, M. Lichtner, R. Menzel, M. Radziunas, D. Skoczowsky, A.G. Vladimirov. Opt. Express, **17**, 19599 (2009). DOI: 10.1364/OE.17.019599
[12] A. Podoskin, V. Golovin, P. Gavrina, D. Veselov, V. Zolotarev, V. Shamakhov, D. Nikolaev, A. Leshko, S. Slipchenko, N. Pikhtin, P. Kopèv. Appl. Optics, **58**, 9089 (2019). DOI: 10.1364/AO.58.009089
[13] A.A. Podoskin, V.S. Golovin, P.S. Gavrina, D.A. Veselov, V.V. Zolotarev, V.V. Shamakhov, D.N. Nikolaev, I.S. Shashkin, S.O. Slipchenko, N.A. Pikhtin, P.S. Kopèv. JOSA B, **37**, 784 (2020). DOI: 10.1364/JOSAB.384971
[14] S.O. Slipchenko, I.S. Shashkin, D.A. Veselov, V.A. Kriychkov, A.E. Kazakova, A.Y. Leshko, V.V. Shamakhov, D.N. Nikolaev, N.A. Pikhtin. J. Light Technol., **40**, 2933 (2022). DOI: 10.1109/JLT.2022.3144663

Translated by E. Potapova